

SPECIAL COLLECTION: APATITE: A COMMON MINERAL, UNCOMMONLY VERSATILE

The crystal structure of turneaureite, $\text{Ca}_5(\text{AsO}_4)_3\text{Cl}$, the arsenate analog of chlorapatite, and its relationships with the arsenate apatites johnbaumite and svabite

CRISTIAN BIAGIONI^{1,*}, FERDINANDO BOSI^{2,3}, ULF HÄLENIUS⁴, AND MARCO PASERO¹

¹Dipartimento di Scienze della Terra, Università di Pisa, Via S. Maria 53, I-56126 Pisa, Italy

²Dipartimento di Scienze della Terra, Sapienza Università di Roma, Piazzale Aldo Moro 5, I-00185 Roma, Italy

³CNR—Istituto di Geoscienze e Georisorse, UOS Roma, Piazzale Aldo Moro 5, I-00185 Roma, Italy

⁴Department of Geosciences, Swedish Museum of Natural History, Box 50007, SE-10405 Stockholm, Sweden

ABSTRACT

The crystal structure of turneaureite, ideally $\text{Ca}_5(\text{AsO}_4)_3\text{Cl}$, was studied using a specimen from the Brattfors mine, Nordmark, Värmland, Sweden, by means of single-crystal X-ray diffraction data. The structure was refined to $R_1 = 0.017$ on the basis of 716 unique reflections with $F_o > 4\sigma(F_o)$ in the $P6_3/m$ space group, with unit-cell parameters $a = 9.9218(3)$, $c = 6.8638(2)$ Å, $V = 585.16(4)$ Å³. The chemical composition of the sample, determined by electron-microprobe analysis, is (in wt%; average of 10 spot analyses): SO_3 0.22, P_2O_5 0.20, V_2O_5 0.01, As_2O_5 51.76, SiO_2 0.06, CaO 41.39, MnO 1.89, SrO 0.12, BaO 0.52, PbO 0.10, Na_2O 0.02, F 0.32, Cl 2.56, $\text{H}_2\text{O}_{\text{calc}}$ 0.58, $\text{O}(\equiv\text{F}+\text{Cl})$ -0.71, total 99.04. On the basis of 13 anions per formula unit, the empirical formula corresponds to $(\text{Ca}_{4.82}\text{Mn}_{0.17}\text{Ba}_{0.02}\text{Sr}_{0.01})_{\Sigma 5.02}(\text{As}_{2.94}\text{P}_{0.02}\text{S}_{0.02}\text{Si}_{0.01})_{\Sigma 2.99}\text{O}_{12}[\text{Cl}_{0.47}(\text{OH})_{0.42}\text{F}_{0.11}]_{\Sigma 1.00}$.

Turneaureite is topologically similar to the other members of the apatite supergroup: columns of face-sharing $M1$ polyhedra running along c are connected through TO_4 tetrahedra with channels hosting $M2$ cations and X anions. Owing to its particular chemical composition, the studied turneaureite can be considered as a ternary calcium arsenate apatite; consequently it has several partially filled anion sites within the anion columns. Polarized single-crystal FTIR spectra of the studied sample indicate stronger hydrogen bonding and less diverse short-range atom arrangements around (OH) groups in turneaureite as compared to the related minerals johnbaumite and svabite. An accurate knowledge of the atomic arrangement of this apatite-remediation mineral represents an improvement in our understanding of minerals able to sequester and stabilize heavy metals such as arsenic in polluted areas.

Keywords: Turneaureite, calcium arsenate, apatite supergroup, crystal structure, infrared spectroscopy, Sweden, Apatite: A common mineral, uncommonly versatile

INTRODUCTION

Calcium arsenate apatites belong to the apatite supergroup, a series of minerals having the general formula $^{IX}M1_2^{VI}M2_3(^{IV}\text{TO}_4)_3X$ (Pasero et al. 2010). Three calcium arsenate members are known: johnbaumite, svabite, and turneaureite, differing for the nature of the X anion, that is $(\text{OH})^-$, F^- , and Cl^- , respectively. Whereas the crystal structures of johnbaumite and svabite were recently investigated (Biagioni and Pasero 2013; Biagioni et al. 2016), the structural features of turneaureite have not been described so far, even if the crystal structure of synthetic $\text{Ca}_5(\text{AsO}_4)_3\text{Cl}$ was reported by Wardojo and Hwu (1996). In addition, natural specimens of turneaureite usually show a complex anion composition, allowing a better understanding of the crystal chemistry of binary and ternary calcium arsenate apatites. Indeed, whereas binary and ternary calcium phosphate apatite samples have been accurately studied (e.g., Hughes et al. 1989, 1990, 2014), few data are available for their arsenate analogs. This paper aims at filling this gap.

Turneaureite was first described by Dunn et al. (1985) from three different localities, i.e., Franklin, New Jersey, U.S.A.; Balmat, New York, U.S.A.; and Långban, Värmland, Sweden, as the arsenate analog of chlorapatite, $\text{Ca}_5(\text{PO}_4)_3\text{Cl}$, and the calcium analog of mimetite, $\text{Pb}_5(\text{AsO}_4)_3\text{Cl}$. Only the specimen from the Swedish locality allowed the full-characterization of the species and was designated as the holotype. Although the symmetry of apatites is typically hexagonal (space group $P6_3/m$), several phases have been reported with lower symmetry (e.g., White et al. 2005; Baikie et al. 2007), sometimes showing superstructure reflections (e.g., Chakhmouradian and Medici 2005). This is particularly true for Cl-bearing apatites. As a matter of fact neither deviation from the hexagonal symmetry nor any superstructure reflections in turneaureite were reported by Dunn et al. (1985). The specimen from Långban has chemical composition $(\text{Ca}_{4.85}\text{Mn}_{0.16}\text{Pb}_{0.02})_{\Sigma 5.03}[(\text{AsO}_4)_{2.42}(\text{PO}_4)_{0.54}]_{\Sigma 2.96}(\text{Cl}_{0.56}\text{F}_{0.39})_{\Sigma 0.95}$, with unit-cell parameters $a = 9.810(4)$, $c = 6.868(4)$ Å, $V = 572.4$ Å³. The crystal structure of synthetic $\text{Ca}_5(\text{AsO}_4)_3\text{Cl}$ was refined by Wardojo and Hwu (1996) in the space group $P6_3/m$, with unit-cell parameters $a = 10.076(1)$, $c = 6.807(1)$ Å, $V = 598.4$ Å³. Dai and Harlow (1991) presented, as a communication at a meeting, the results of the single-crystal X-ray diffraction study for the

* E-mail: biagioni@dst.unipi.it

Special collection papers can be found online at <http://www.minsocam.org/MSA/AmMin/special-collections.html>.

three natural calcium arsenate apatites, but to our knowledge the results of their work were never published.

An understanding of the crystal structure of As-rich minerals is useful in environmental remediation (e.g., Rakovan and Pas-teris 2015), thus we carried out a combined chemical, structural, and spectroscopic study of turneaureite from Nordmark, Värmland, Sweden. The present data, in conjunction with data from johnbaumite and svabite (Biagioni and Pasero 2013; Biagioni et al. 2016), provide the basis for a comparative analysis of the crystal-chemical features of the three calcium arsenate minerals with the apatite structure.

EXPERIMENTAL METHODS

The studied specimen (catalog number NRM19532695) is from the Brattfors mine (latitude 59.83°N, longitude 14.12°E), Nordmark ore field, Filipstad, Värmland, Sweden. In this area there are about 20 small mines and prospects, which have been worked mainly for magnetite ore (e.g., Magnusson 1929). The studied specimen of turneaureite consists of a fine-grained, irregularly fine-banded, metamorphosed siliceous carbonate rock, mainly composed of Mn-bearing calcite. Alleghanyite, jacobsonite, and tephroite occur as small (<0.5 mm) rounded grains together with katoptrite and turneaureite in the calcite matrix. Grains of turneaureite (up to 3 mm) are rounded or short prismatic to almost fibrous in habit, whereas katoptrite grains (up to 2 mm long) are typically lath-shaped. Very rare rounded grains (<1 mm) of magnusonite are also observed. Dark red aggregates of alleghanyite cover up to 1 cm² large areas in some micro-fissures.

Electron microprobe analyses were obtained by wavelength-dispersive spectroscopy (WDS mode) with a Cameca SX50 instrument at the "Istituto di Geologia Ambientale e Geoingegneria, CNR" of Rome, Italy, using the following analytical conditions: accelerating voltage 15 kV, beam current 15 nA, nominal beam diameter 1 μm. Counting time for one spot analysis was 20 s per peak. Standards (element, emission line) are: baryte (BaLa, SKα), apatite (PKα), GaAs (AsLa), wollastonite (CaKα, SiKα), vanadinite (VKα), rhodonite (MnKα), celestine (SrKα), galena (PbMα), jadeite (NaKα), phlogopite (FKα), and sylvite (ClKα). The PAP routine was applied (Pouchou and Pichoir 1991) for correction of recorded raw data. Ten spot analyses were performed; the studied grain was found to be homogeneous. Chemical data are given in Table 1; the chemical formula, based on 13 anions per formula unit, is (Ca_{4.82}Mn_{0.17}Ba_{0.02}Str_{0.01})_{25.02}(As_{2.94}P_{0.02}Si_{0.01})_{22.99}O₁₂[Cl_{0.47}(OH)_{0.42}F_{0.11}]_{21.00}.

Polarized single-crystal infrared spectra of turneaureite were recorded with a Bruker Vertex 70 microscope spectrometer equipped with a halogen lamp source, a KBr beam-splitter, a holographic ZnSe polarizer, and a midband MCT detector. The crystal was oriented by morphology and optical microscopy and was doubly polished parallel to the a-c axis plane. The thickness of the single-crystal absorber was 38 μm. Polarized absorption spectra were acquired parallel (E||E) and perpendicular (E||O) to the c-axis over the wavenumber range 600–5000 cm⁻¹ with a resolution of 2 cm⁻¹ during 32 cycles. The spectral region of the O–H stretching bands of the recorded single-crystal spectra was fitted using the PeakFit 4.12 software (Jandel) assuming Gaussian peak shapes.

A crystal fragment (230 × 230 × 100 μm in size) was selected for the single-crystal X-ray diffraction study. Intensities were collected using a Bruker Smart Breeze diffractometer (50 kV, 30 mA) equipped with a CCD 4k low-noise area detector. Graphite-monochromatized MoKα radiation was used. The detector-to-crystal working distance was 50 mm; 558 frames were collected in ω and φ scan modes in 0.5° slices; exposure time was 10 s per frame. The data were integrated and corrected for Lorentz and polarization, background effects, and absorption using the package of softwares Apex2 (Bruker AXS Inc. 2004), resulting in a set of 753 independent reflections. The refinement of unit-cell parameters constrained to hexagonal symmetry gave *a* = 9.9218(3), *c* = 6.8638(2) Å, *V* = 585.16(4) Å³. The statistical tests on the distribution of |E| values (|E² - 1| = 1.019) and the systematic absences suggested the space group *P*6₃/*m*.

The crystal structure was refined starting from the atomic coordinates of chlorapatite (Hughes et al. 1989) using SHELXL-2014 (Sheldrick 2015). Scattering curves for neutral atoms were taken from the *International Tables for Crystallography* (Wilson 1992). The site occupation factors (s.o.f.) of the three cation and four anion sites were initially refined using the following scattering curves: Ca at the *M1* and *M2* sites; As at the *T* site; O at the O1, O2, O3 sites and Cl at the *X* site. Owing to the complex anion chemistry, the position of the latter site was found through difference-Fourier map that showed the presence of a maximum at (0, 0, ¼). After a few cycles of isotropic refinement, the *R*₁ converged to 0.079. To account for the occurrence of other elements

substituting for Ca, the s.o.f. of *M1* and *M2* were refined using the scattering curves of Ca vs. Mn and Ca vs. Ba, respectively. Only a minor improvement of the refinement was observed. After the introduction of the anisotropic displacement parameters for cations, the *R*₁ converged to 0.054. Assuming an anisotropic model also for the O1, O2, and O3 positions, the *R*₁ value converged to 0.047. The displacement parameter of the *X* anion was refined isotropically. Indeed, the anisotropic refinement of the displacement parameter of the *X* anion resulted in a very high *U* value [in particular *U*³³, i.e., 0.262(6) Å²], suggesting the replacement of Cl by lighter atoms (in agreement with chemical data) and the structural disorder affecting the column anions. Likely, these high values of the anisotropic displacement parameters could mask the occurrence of several partially occupied positions along the columns. Consequently, notwithstanding the good *R* value obtained using an anisotropic description of the displacement parameter of the *X* position (i.e., *R*₁ = 0.023), an isotropic model was preferred. In this way, a very high residual of 7.5 e/Å³ at (0, 0, 0.33) was found. By adding this additional position (named *Xb*), constraining the isotropic *U* value of *Xa* and *Xb* to be equal, and freely refining their s.o.f., the *R*₁ converged to 0.018. The refined site scattering indicated the occurrence of about 5.5 and 7.8 electrons per formula unit at *Xa* and *Xb*, respectively. The *Xb* position was assumed to be occupied by Cl only, owing to the longer *M2*–*Xb* distance, whereas *Xa* was assumed to have a mixed (OH, Cl, F) occupancy. The proposed site population, taking into account the site multiplicity, was (OH)_{0.42}F_{0.11}Cl_{0.06} and Cl_{0.41} at *Xa* and *Xb*, respectively. The highest maximum residual was 1.14 e/Å³ at (0, 0, 0.40); this position is similar to the split Cl site found by Hughes et al. (1990) in ternary apatites. Consequently, we added this further position, labeled as *Xc*, assuming for it a partial occupancy by Cl only, and removing the minor amount of this element from the *Xa* site. The refinement converged to *R*₁ = 0.0172 for 716 unique reflections with *F*_o > 4 σ(*F*_o) (0.0185 for all 753 reflections) and 42 refined parameters. The chemical formula derived from the structure refinement (SREF) is (Ca_{4.92}Ba_{0.05}Mn_{0.03})(AsO₄)₃[Cl_{0.47}(OH)_{0.42}F_{0.11}]. Details of data collection and refinement are given in Table 2. Fractional atom coordinates, site occupancy factors, and isotropic or equivalent isotropic displacement parameters are reported in Table 3, whereas Table 4 gives anisotropic displacement parameters. Finally, Table 5 reports selected bond distances, and Table 6 shows the bond-valence calculations obtained using the bond-valence parameters of Brese and O'Keeffe (1991). The CIF is available as supplementary material¹.

CRYSTAL STRUCTURE DESCRIPTION

General features, cation coordination, and site population

The crystal structure of turneaureite is topologically similar to those of the other members of the apatite supergroup. It is composed by columns of face-sharing *M1*-centered polyhedra running along *c*; those polyhedra can be described as tricapped trigonal prisms. Adjacent columns are connected by *TO*₄ tetrahedra through corner-sharing. The *M1* and *M2* sites are Ca-dominant sites, with only a minor replacement by other cations, in agreement with chemical data. Refined site scattering at *M1* (20.0 electrons) suggests only negligible replacement by heavier elements; consequently this site has a virtually pure Ca site population. The average <*M1*–O> distance is 2.579 Å, to be compared with 2.584 Å reported by Wardojo and Hwu (1996) for synthetic Ca₅(AsO₄)₃Cl and 2.549 Å for chlorapatite studied by Hughes et al. (1989). Bond valence sum (BVS) at *M1*, calculated using the proposed site population, is 1.98 valence units (v.u.). The *M2* site has a sevenfold coordination, with <*M2*–φ> = 2.529 Å, compared with 2.505 and 2.493 Å for synthetic Ca₅(AsO₄)₃Cl and chlorapatite, respectively. The *M2* site scattering (20.7 e) agrees with the site population (Ca_{0.93}Mn_{0.06}Ba_{0.01}). The BVS at *M2* is 2.00 v.u. The site population of the *M1*+*M2* sites, taking into account the site multiplicity, is consistent with (Ca_{4.79}Mn_{0.18}Ba_{0.03}), in agreement with electron-microprobe data. Finally, the *T* site is occupied by As⁵⁺, with minor substitutions of P⁵⁺, S⁶⁺, and Si⁴⁺. The average

¹Deposit item AM-17-106041, CIF. Deposit items are free to all readers and found on the MSA web site, via the specific issue's Table of Contents (go to http://www.minsocam.org/MSA/AmMin/TOC/2017/Oct2017_data/Oct2017_data.html).

TABLE 1. Electron-microprobe data (mean of 10 spot analyses, in wt%) of turneaureite, estimated standard deviation (e.s.d.), and atoms per formula unit (apfu), on the basis of 13 anions

| Oxide | wt% | Range | e.s.d. | apfu |
|------------------------------------|-------|-------------|--------|-------|
| SO ₃ | 0.22 | 0.02–1.10 | 0.31 | 0.018 |
| P ₂ O ₅ | 0.20 | 0.12–0.26 | 0.08 | 0.018 |
| V ₂ O ₅ | 0.01 | 0.00–0.06 | 0.02 | 0.001 |
| As ₂ O ₃ | 51.76 | 50.27–52.40 | 0.78 | 2.942 |
| SiO ₂ | 0.06 | 0.03–0.09 | 0.02 | 0.007 |
| CaO | 41.39 | 40.45–41.89 | 0.63 | 4.821 |
| MnO | 1.89 | 1.54–3.37 | 0.65 | 0.174 |
| SrO | 0.12 | 0.05–0.28 | 0.08 | 0.008 |
| BaO | 0.52 | 0.11–2.38 | 0.82 | 0.022 |
| PbO | 0.10 | 0.00–0.24 | 0.08 | 0.003 |
| Na ₂ O | 0.02 | 0.00–0.06 | 0.02 | 0.004 |
| F | 0.32 | 0.11–0.56 | 0.14 | 0.110 |
| Cl | 2.56 | 2.15–2.84 | 0.21 | 0.472 |
| H ₂ O ^(calc) | 0.58 | | | 0.421 |
| O=F+Cl | –0.71 | | | |
| Total | 99.04 | | | |

Note: H₂O was calculated with the assumption (Cl+F+OH) = 1 apfu.

TABLE 2. Crystal data and summary of parameters describing data collection and refinement for turneaureite

| Crystal data | |
|---|---|
| Crystal size (mm) | 0.23 × 0.23 × 0.10 |
| Cell setting, space group | Hexagonal, <i>P6₃/m</i> |
| <i>a</i> , <i>c</i> (Å) | 9.9218(3), 6.8638(2) |
| <i>V</i> (Å ³) | 585.16(4) |
| <i>Z</i> | 2 |
| Data collection and refinement | |
| Radiation, wavelength (Å) | MoKα, 0.71073 |
| Temperature (K) | 298 |
| Detector-to-sample distance (mm) | 50 |
| Number of frames | 558 |
| Rotation width per frame (°) | 0.5 |
| Maximum observed 2θ (°) | 65.05 |
| Measured reflections | 2720 |
| Unique reflections | 753 |
| Reflections with <i>F_o</i> > 4σ(<i>F_o</i>) | 716 |
| <i>R_{int}</i> after absorption correction | 0.0156 |
| <i>R_w</i> | 0.0146 |
| Range of <i>h</i> , <i>k</i> , <i>l</i> | –8 ≤ <i>h</i> ≤ 13 –15 ≤ <i>k</i> ≤ 10 –10 ≤ <i>l</i> ≤ 5 |
| <i>R_i</i> [<i>F_o</i> > 4σ(<i>F_o</i>)] | 0.0172 |
| <i>R_i</i> (all data) | 0.0185 |
| w <i>R₂</i> (on <i>F_o</i>) | 0.0447 |
| Goof | 1.108 |
| Number of l.s. parameters | 42 |
| Maximum and minimum residual | 0.75 (at 0.56 Å from <i>M2</i>) –0.88 (at 0.74 Å from <i>M2</i>) |

<*T*–*O*> distance is 1.678 Å, a little longer than the bond distances observed in johnbaumite and svabite (1.671 and 1.674 Å, respectively; Biagioni and Pasero 2013; Biagioni et al. 2016) and close to that reported for synthetic Ca₅(AsO₄)₃Cl (1.682 Å) by Wardojo and Hwu (1996) and for johnbaumite from Franklin (1.70 Å) by Henderson et al. (2009). The BVS at *T* is 5.10 v.u.

The anion columns

The studied specimen can be classified as turneaureite, because Cl is the dominant column anion. Actually, this sample could be defined as a ternary calcium arsenate apatite, with chemical composition Turn₄₇John₄₂Svab₁₁.

Three sites in the [001] columns were located, at coordinates (0, 0, ¼), (0, 0, 0.31), and (0, 0, 0.37). Whereas in end-member (OH)-apatites, the hydroxyl group is displaced from the (0, 0, ¼) position, being disordered 0.35 Å above or below the mirror plane (e.g., Hughes et al. 1989; Biagioni and Pasero 2013), in turneaureite the (OH) groups have been located at

TABLE 3. Site occupancy factors (s.o.f.), fractional atom coordinates, and isotropic (*) or equivalent isotropic displacement parameters (in Å²) for turneaureite

| Site | Wyckoff position | s.o.f. | <i>x/a</i> | <i>y/b</i> | <i>z/c</i> | <i>U_{eq/iso}</i> |
|-----------|------------------|---|-------------|-------------|-------------|---------------------------|
| <i>M1</i> | 4 <i>f</i> | Ca _{0.328(3)} Mn _{0.005(3)} | ½ | ¼ | 0.00395(8) | 0.01344(14) |
| <i>M2</i> | 6 <i>h</i> | Ca _{0.491(1)} Ba _{0.009(1)} | 0.01102(6) | 0.26117(7) | ¼ | 0.02306(18) |
| <i>T</i> | 6 <i>h</i> | As _{0.50} | 0.37437(3) | 0.40457(3) | ¼ | 0.01006(8) |
| <i>O1</i> | 6 <i>h</i> | O _{0.50} | 0.5020(2) | 0.3416(2) | ¼ | 0.0198(4) |
| <i>O2</i> | 6 <i>h</i> | O _{0.50} | 0.4663(2) | 0.6012(2) | ¼ | 0.0171(3) |
| <i>O3</i> | 12 <i>i</i> | O _{1.00} | 0.25644(16) | 0.34708(18) | 0.44470(19) | 0.0217(3) |
| <i>Xa</i> | 2 <i>a</i> | (OH) _{0.070} F _{0.018} | 0 | 0 | ¼ | 0.0160(5)* |
| <i>Xb</i> | 4 <i>e</i> | Cl _{0.068} | 0 | 0 | 0.3055(6) | 0.0160(5)* |
| <i>Xc</i> | 4 <i>e</i> | Cl _{0.010} | 0 | 0 | 0.370(4) | 0.0160(5)* |

Note: *U_{eq}* is defined as one third of the trace of the orthogonalized *U^{ij}* tensor.

TABLE 4. Anisotropic displacement parameters (in Å²) for turneaureite

| Site | <i>U¹¹</i> | <i>U²²</i> | <i>U³³</i> | <i>U²³</i> | <i>U¹³</i> | <i>U¹²</i> |
|-----------|-----------------------|-----------------------|-----------------------|-----------------------|-----------------------|-----------------------|
| <i>M1</i> | 0.01587(18) | 0.01587(18) | 0.0086(2) | 0 | 0 | 0.00794(9) |
| <i>M2</i> | 0.0162(2) | 0.0346(3) | 0.0117(2) | 0 | 0 | 0.0077(2) |
| <i>T</i> | 0.01083(11) | 0.01054(11) | 0.01045(11) | 0 | 0 | 0.00658(8) |
| <i>O1</i> | 0.0230(9) | 0.0338(10) | 0.0146(7) | 0 | 0 | 0.0233(9) |
| <i>O2</i> | 0.0178(8) | 0.0098(7) | 0.0225(8) | 0 | 0 | 0.0060(6) |
| <i>O3</i> | 0.0188(6) | 0.0351(7) | 0.0156(6) | 0.0097(6) | 0.0066(5) | 0.0168(6) |

TABLE 5. Selected bond distances (in Å) for turneaureite

| | | | | | | | | |
|--------------------------|----------------|------------|--------------------------|----------------|------------|-------------------------|----------------|------------|
| <i>M1</i> | <i>O1</i> (×3) | 2.3800(13) | <i>M2</i> | <i>O3</i> (×2) | 2.3159(13) | <i>T</i> | <i>O1</i> | 1.6681(18) |
| | <i>O2</i> (×3) | 2.4609(14) | | <i>O2</i> | 2.345(2) | | <i>O3</i> (×2) | 1.6772(13) |
| | <i>O3</i> (×3) | 2.8953(16) | | <i>O3</i> (×2) | 2.5232(15) | | <i>O2</i> | 1.6909(17) |
| | | | | <i>Xa</i> | 2.5384(7) | | | |
| | | | | <i>Xb</i> | 2.5669(9) | | | |
| | | | | <i>Xc</i> | 2.669(9) | | | |
| | | | | <i>O1</i> | 3.121(2) | | | |
| < <i>M1</i> – <i>O</i> > | 2.579 | | < <i>M2</i> – <i>O</i> > | 2.529 | | < <i>T</i> – <i>O</i> > | 1.678 | |

TABLE 6. Weighted bond valences for turneaureite, in valence units (v.u.)

| Site | <i>O1</i> | <i>O2</i> | <i>O3</i> | <i>Xa</i> | <i>Xb</i> | <i>Xc</i> | Σ cations |
|-----------|-----------------------------------|-----------------------------------|---------------------|--------------------|--------------------|--------------------|-----------|
| <i>M1</i> | ^{3x} –0.32 ^{×2} | ^{3x} –0.26 ^{×2} | ^{3x} –0.08 | | | | 1.98 |
| <i>M2</i> | 0.04 | 0.36 | ^{2x} –0.39 | 0.11 ^{×3} | 0.25 ^{×3} | 0.02 ^{×3} | 2.00 |
| <i>T</i> | 1.31 | 1.23 | ^{2x} –1.28 | | | | 5.10 |
| Σ anions | 1.99 | 2.11 | 1.97 | 0.33 | 0.75 | 0.06 | |

Notes: Left and right superscripts indicate the number of equivalent bonds involving cations and anions, respectively. For sites with mixed occupancy, the bond valences have been weighted according to the proposed site population: *M1* = Ca_{1.00}; *M2* = Ca_{0.93}Mn_{0.06}Ba_{0.01}.

the *Xa* position lying on the mirror plane. A minor substitution of (OH) by F is proposed. The *Xb* and *Xc* sites have been assumed to be occupied by Cl only. Actually, such split sites are inserted to model an electron density that is continuously distributed along the anion column and around the mirror plane, constrained by the necessity to avoid unrealistically short anion–anion distances.

In any column, there are five possible anion sites: (1) *Xa*, located on the mirror plane; (2 and 3) *Xb*, located 0.38 Å above (hereafter *Xb_a*, where subscript *a* stands for above) and 0.38 Å below (*Xb_b*, where subscript *b* stands for below) the mirror plane; and (4 and 5) *Xc*, located 0.83 Å above (*Xc_a*) and below (*Xc_b*) the mirror plane. Figure 1 show the anion–anion distances in the studied turneaureite. Owing to the necessity to avoid short anion–anion contacts, only some configurations are possible, confirming that complete disordering along anion columns is not realistic. Consequently, there could be anion ordering within individual columns and disordering among the column themselves, thus giving rise to completely disordered hexagonal structures (e.g., Hughes et al. 1989).

**Anion associated with mirror plane
at $z = \frac{3}{4}$**

| Anion associated with mirror plane at $z = \frac{1}{4}$ | | Xa | Xb _a | Xb _b | Xc _a | Xc _b |
|--|--|------|-----------------|-----------------|-----------------|-----------------|
| Xa | | 3.43 | 3.81 | 3.05 | 4.26 | 2.61 |
| Xb _a | | 3.05 | 3.43 | 2.67 | 3.88 | 2.23 |
| Xb _b | | 3.81 | 4.19 | 3.43 | 4.64 | 2.99 |
| Xc _a | | 2.61 | 2.99 | 2.23 | 3.43 | 1.78 |
| Xc _b | | 4.26 | 4.64 | 3.88 | 5.08 | 3.43 |

FIGURE 1. Anion–anion distances (in angstroms) for column anions. Same labels as in the text. Gray cells indicate configurations not allowed owing to too short interionic distances.

Bond strain analysis

Bosi (2014) demonstrated the occurrence of systematic errors in bond valence calculations incident at the mixed occupancy sites. This type of error is very insidious because it can give rise to a false indication of the presence of steric strain. However, as the systematic errors introduced into the weighted BVS of turneaureite (Table 6) have been estimated to be small (<0.05 v.u.), the difference between BVS and expected weighted atomic valence can be interpreted in terms of bond strain (Brown 2016). In detail, the anions at Xa may be considered as underbonded, because its BVS is smaller than the expected value (0.33 and 0.53 v.u., respectively). On the other hand, Xb may be considered as overbonded, because its BVS is larger than the expected value (0.75 and 0.41 v.u., respectively). Regarding the Xc site, its BVS agrees with the expected value (0.06 v.u.). The above-mentioned deviations (bond strain) from the expected bond valence sum values are likely related to the disorder in the actual position of the column anions and possibly to the unresolved splitting of the M2 site.

DISCUSSION

Chlorine position in turneaureite

Hughes et al. (1989) determined the anion positions in end-member calcium phosphate apatites and postulated that the anion positions in binary and ternary (F–OH–Cl) apatites would be impossible to predict. Indeed, in agreement with these authors, an extensive rearrangement of the end-member anion configurations may occur in ternary apatites to accommodate the large Cl[−] anion. In chlorapatite, Cl is located at (0, 0, 0.44), 1.2 Å above and below the mirror plane located at (0, 0, $\frac{1}{4}$) (Hughes et al. 1989); in synthetic Ca₅(AsO₄)₃Cl, Cl is at (0, 0, 0.37), 0.84 Å above and below the mirror plane (Wardojo and Hwu 1996). In

ternary phosphate apatites, a 0.4 Å shift of the Cl[−] anion toward the mirror plane was observed by Hughes et al. (1990). Such a shift is accompanied by a splitting of the M2 position as a function of the neighboring anion to which M2-hosted cation is bonded. In some cases, the ordering of Cl and (OH) in anion columns could result in a lowering of symmetry, from $P6_3/m$ to $P2_1/b$ with a doubling of the **b** axis (Chakhmouradian and Medici 2006).

In the turneaureite studied, only the first phenomenon, i.e., the shift of Cl, occurs, whereas no hints of the occurrence of a doubling of the *b* parameter were observed. The splitting of the M2 site was not resolved, even if the U^{22} value is definitely larger than the corresponding value at M1 and those reported for M2 sites in johnbaumite and svabite (Biagioni and Pasero 2013; Biagioni et al. 2016), thus suggesting a possible positional disorder of this site in the {0001} plane.

In the studied sample, Cl is mainly located at (0, 0, 0.31), corresponding to a shift of 0.44 Å with respect to the Cl position in synthetic Ca₅(AsO₄)₃Cl. Another split position, having a low s.o.f., occurs at (0, 0, 0.37), corresponding to the coordinates of the Cl in the synthetic compound. This behavior is similar to that reported by Hughes et al. (1990) during their study of ternary apatites. Indeed they located Cl at (0, 0, 0.368), shifted 0.4 Å toward the mirror plane with respect to near to end-member chlorapatite; in addition, they found another split site, having a low site occupancy, at coordinates corresponding to that of Cl in chlorapatite, i.e., (0, 0, 0.44).

The Ca–Cl distances in turneaureite, i.e., 2.57 (M2–Xb) and 2.67 Å (M2–Xc), are similar to those given by Hughes et al. (1990) for ternary apatites, i.e., 2.63 and 2.70 Å for the two split Ca2 positions, in keeping with the chemical complexity of the turneaureite studied. These distances are definitely shorter than those reported for synthetic Ca₅(AsO₄)₃Cl and for chlorapatite, both showing Ca–Cl distances of ~2.76 Å (Hughes et al. 1989; Wardojo and Hwu 1996), in keeping with the shift of Cl toward the mirror plane in apatites having a complex anion chemistry and the unresolved splitting of the M2 site.

Comparison with johnbaumite and svabite

The refinement of the crystal structure of turneaureite, in conjunction with data from Biagioni and Pasero (2013) and Biagioni et al. (2016), completes the triptych of natural calcium arsenate apatites, allowing important comparison of their structural features.

Natural samples generally have non-ideal (non-end-member) compositions. Indeed, only the johnbaumite composition studied by Biagioni and Pasero (2013) was close to the ideal Ca₅(AsO₄)₃(OH) formula, having only negligible amounts of Cl and with F being below the detection limit. The sample of svabite, on the contrary, contains significant amounts of (OH) replacing F. Concerning cation substitutions, Ca was replaced by Pb and Mn only in svabite and turneaureite, respectively. Phosphorus-to-arsenic substitution is trivial in all the studied samples (up to 0.04 apfu in johnbaumite).

Unit-cell parameters of johnbaumite and svabite are similar, with $a = 9.72$, $c = 6.96$ Å, $V = 570.4$ Å³ for the former and $a = 9.73$, $c = 6.98$ Å, $V = 572.1$ Å³ for the latter. The unit-cell volume increase of svabite is only related to minor Pb replacing Ca. Indeed, the size of (OH)[−] is slightly larger than F[−] and

consequently the unit-cell volume of johnbaumite should be larger than that of svabite. The unit-cell volume of turneaureite is significantly larger, i.e., 585.2 \AA^3 ($\Delta V = +2.3$ and $+2.6\%$ with respect to svabite and johnbaumite, respectively). Notably there is an expansion of the a parameter ($a = 9.92 \text{ \AA}$, $\Delta a \sim +2\%$) accompanied by a contraction of the c parameter ($c = 6.86 \text{ \AA}$, $\Delta c \sim -1.6\%$); this behavior is more evident in synthetic $\text{Ca}_5(\text{AsO}_4)_3\text{Cl}$, having $a = 10.076 \text{ \AA}$ ($\Delta a \sim +3.5\%$) and $c = 6.807 \text{ \AA}$ ($\Delta c \sim -2.3\%$). This could accommodate an increase in the diameter of the anion columns (Fig. 2), favoring the accommodation of the large Cl^- anion, as indicated by the larger $M2-M2$ distance in turneaureite (4.40 \AA) with respect to those observed in johnbaumite and svabite ($4.11-4.12 \text{ \AA}$). Indeed, as the size of the X anion increases, the tunnels become wider through reduction in the metaprisism twist angle φ (e.g., White and Dong 2003; White et al. 2005), defined as the angle $\text{O1}-M1-\text{O2}$ projected on (001) (White and Dong 2003; Lim et al. 2011). This angle is used for the assessment of the distortion of the apatite structure from an ideal hexagonal close packing of oxygen atoms. The metaprisism twist angle in turneaureite, calculated according to the formula proposed by Henderson et al. (2009), is 16.4° , definitely smaller than the corresponding angles observed in johnbaumite (21.1° , Biagioni and Pasero 2013) and svabite (21.5° , Biagioni et al. 2016), but in agreement with the expansion of the anion columns in the (001) plane.

Fourier transform infrared spectroscopy (FTIR) of turneaureite

The infrared spectra of turneaureite are very similar to those reported for svabite and johnbaumite (Biagioni et al. 2016) and display strong absorption bands related to vibrational modes in AsO_4 -tetrahedra in the range $750-950 \text{ cm}^{-1}$ and distinct absorption related to O-H stretching modes in the range $3450-3600 \text{ cm}^{-1}$. As in spectra of the related minerals, the O-H stretching band is polarized in E||c because of O-H dipole alignments along the crystallographic c axis. The recorded FTIR E||c (E||E) spectrum of turneaureite in the O-H stretching region is compared with those of svabite and johnbaumite in Figure 3. Whereas the positions of the O-H stretching bands are almost identical in svabite and johnbaumite (Biagioni et al. 2016), they are shifted toward lower wavenumbers by $5-15 \text{ cm}^{-1}$ in turneaureite, thus indicating stronger hydrogen bonding. In addition, the intensity of the high-energy component of the O-H stretch-

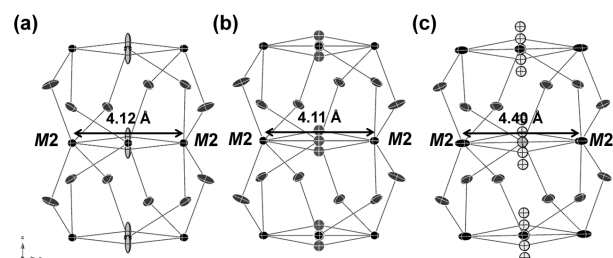


FIGURE 2. Comparison among the anion columns in johnbaumite (a), svabite (b), and turneaureite (c). The $M2-M2$ distances are shown. Atoms are drawn as thermal ellipsoids. Symbols: black = $M2$ site; dark gray = O sites; light gray = (OH)-dominant sites; gray = F-dominant sites; white = Cl-dominant sites.

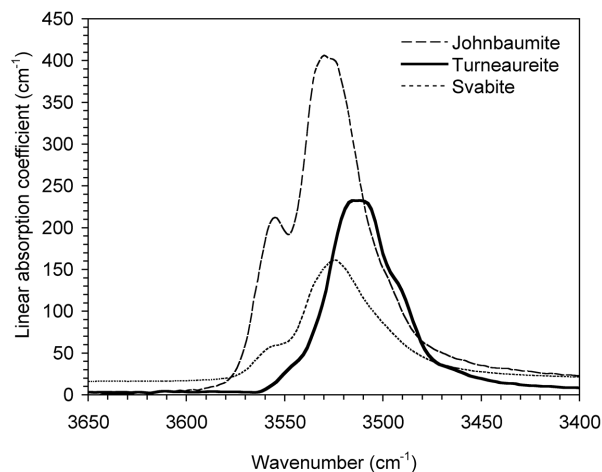


FIGURE 3. Infrared E||E (E||c) spectra of turneaureite (thick line) in the O-H stretching region compared with those of johnbaumite (thin broken line) and svabite (thin dotted line) (Biagioni et al. 2016).

ing region observed in spectra of johnbaumite and svabite at $\sim 3560 \text{ cm}^{-1}$ is strongly reduced in the turneaureite spectra. This suggests less diverse short-range atom arrangements around the (OH) groups in turneaureite compared to the two related minerals. Using the IR method for determining the (OH) concentration in apatite (Wang et al. 2011), the H_2O content in the turneaureite specimen should be close to $0.28 \text{ wt}\%$, which is lower than the $0.58 \text{ wt}\%$ calculated for the empirical formula on the basis of electron-microprobe analysis. As in svabite and johnbaumite (Biagioni et al. 2016), the calculated H_2O concentration is approximately one half of that estimated from chemical data.

IMPLICATIONS

The occurrence of arsenic in surface and groundwaters in several localities worldwide (e.g., in southeastern Asia; Charlet and Polya 2006) emphasize the importance of calcium arsenate apatites as potential sequestrators and stabilizers of arsenic from polluted water (e.g., Magalhães and Williams 2007; Liu et al. 2014). To explore their possible application in environmental remediation (e.g., Rakovan and Pasteris 2015), knowledge of their crystal chemistry is mandatory, because the atomic arrangement of their crystal structure strongly affects physical properties.

In addition, the complex anion chemistry of the turneaureite studied in this work, showing the simultaneous presence of Cl, (OH), and minor F as column anions, is particularly intriguing. Apatites are among the few minerals showing anion substitution series. Owing to the different sizes of F, (OH), and Cl, as well as to the steric interactions among those anions in the anion columns, particularly complex atomic arrangements could result. As stressed by Hughes et al. (2014), despite the widespread interest in apatites and the dependence of all their properties on the atomic arrangements, the crystal structures of binary and ternary apatites are not well understood as the anion distribution is not predictable from the structures of end-members. Consequently, several studies have been focused on the atomic arrangements in the anion columns (e.g., Hughes 2015). With respect to synthetic $\text{Ca}_5(\text{AsO}_4)_3\text{Cl}$ (Wardojo and Hwu 1996), where only Cl was pres-

ent, the studied turneaureite represents a ternary arsenate apatite that offers the possibility to describe the anion substitution series between turneaureite itself and the two other arsenate apatites (johnbaumite and svabite). The results show a Cl shifting toward the mirror planes, similar to that reported in ternary calcium phosphate apatites (Hughes et al. 1990).

ACKNOWLEDGMENTS

We thank Marcello Serracino who assisted us during electron-microprobe analysis. M.P. acknowledges the financial support from the University of Pisa (PRA_2015_0028). Fernando Cámara, Anthony R. Kampf, and an anonymous reviewer helped us improving the paper.

REFERENCES CITED

- Baikie, T., Mercier, P.H.J., Elcombe, M.M., Kim, J.Y., Le Page, Y., Mitchell, L.D., White, T.J., and Whitfield, P.S. (2007) Triclinic apatites. *Acta Crystallographica*, B63, 251–256.
- Biagioni, C., and Pasero, M. (2013) The crystal structure of johnbaumite, $\text{Ca}_5(\text{AsO}_4)_3\text{OH}$, the arsenate analogue of hydroxylapatite. *American Mineralogist*, 98, 1580–1584.
- Biagioni, C., Bosi, F., Hälenius, U., and Pasero, M. (2016) The crystal structure of svabite, $\text{Ca}_5(\text{AsO}_4)_3\text{F}$, an arsenate member of the apatite supergroup. *American Mineralogist*, 101, 1750–1755.
- Bosi, F. (2014) Bond valence at mixed occupancy sites. I. Regular polyhedra. *Acta Crystallographica*, B70, 864–870.
- Brese, N.E., and O’Keeffe, M. (1991) Bond-valence parameters for anion-anion bonds in solids. *Acta Crystallographica*, B48, 152–154.
- Brown, I.D. (2016) The chemical bond in inorganic chemistry: the bond valence model. Series: International Union of Crystallography Monographs on Crystallography, 12, 352 pp. Oxford University Press, U.K.
- Bruker AXS Inc. (2004) APEX 2. Bruker Advanced X-ray Solutions. Madison, Wisconsin.
- Chakmouradian, A.R., and Medici, L. (2006) Clinohydroxylapatite: a new apatite-group mineral from northwestern Ontario (Canada), and new data on the extent of Na-S substitution in natural apatites. *European Journal of Mineralogy*, 18, 105–112.
- Charlet, L., and Poly, D.A. (2006) Arsenic in shallow, reducing groundwaters in Southern Asia: an environmental health disaster. *Elements*, 2, 91–96.
- Dai, Y.S., and Harlow, G.E. (1991) Structural relationships of arsenate apatites with their anion-devoid intermetallic phase Ca_5As_3 . *Geological Society of America Annual Meeting, Program and Abstracts*, 23, A219.
- Dunn, P.J., Petersen, E.U., and Peacor, D.R. (1985) Turneaureite, a new member of the apatite group from Franklin, New Jersey, Balmat, New York and Långban, Sweden. *Canadian Mineralogist*, 23, 251–254.
- Henderson, C.M.B., Bell, A.M.T., Charnock, J.M., Knight, K.S., Wendlandt, R.F., Plant, D.A., and Harrison, W.J. (2009) Synchrotron X-ray absorption spectroscopy and X-ray powder diffraction studies of the structure of johnbaumite $[\text{Ca}_{10}(\text{AsO}_4)_6(\text{OH},\text{F})_2]$ and synthetic Pb-, Sr- and Ba-arsenate apatites and some comments on the crystal chemistry of the apatite structure type in general. *Mineralogical Magazine*, 73, 433–455.
- Hughes, J.M. (2015) The many facets of apatite. *American Mineralogist*, 100, 1033–1039.
- Hughes, J.M., Cameron, M., and Crowley, K.D. (1989) Structural variation in natural F, OH, and Cl apatites. *American Mineralogist*, 74, 870–876.
- Hughes, J.M., Cameron, M., and Crowley, K.D. (1990) Crystal structures of natural ternary apatites: solid solution in the $\text{Ca}_5(\text{PO}_4)_3\text{X}$ (X = F, OH, Cl) system. *American Mineralogist*, 75, 295–304.
- Hughes, J.M., Nekvasil, H., Ustunisik, G., Lindsley, D.H., Coraor, A.E., Vaughn, J., Phillips, B.L., McCubbin, F.M., and Woerner, W.R. (2014) Solid solution in the fluorapatite-chlorapatite binary system: High-precision crystal structure refinements of synthetic F-Cl apatite. *American Mineralogist*, 99, 369–376.
- Lim, S.C., Baikie, T., Pramana, S.S., Smith, R., and White, T.J. (2011) Apatite metapristm twin angle (ϕ) as a tool for crystallochemical diagnosis. *Journal of Solid State Chemistry*, 184, 2978–2986.
- Liu, J., Huang, X., Liu, J., Wang, W., Zhang, F., and Dong, F. (2014) Experimental and model studies on comparison of As(III and V) removal from synthetic acid mine drainage by bone char. *Mineralogical Magazine*, 78, 73–89.
- Magalhães, M.C.F., and Williams, P.A. (2007) Apatite group minerals: solubility and environmental remediation. In T.M. Letcher, Ed., *Thermodynamics, Solubility and Environmental Issues*, pp. 327–342. Elsevier, New York.
- Magnusson, N.H. (1929) The Nordmark ore district. *Sveriges Geologiska Undersökning*, Ca 13, 98 p. (in Swedish).
- Pasero, M., Kampf, A.R., Ferraris, C., Pekov, I.V., Rakovan, J., and White, T.J. (2010) Nomenclature of the apatite supergroup minerals. *European Journal of Mineralogy*, 22, 163–179.
- Pouchou, J.L., and Pichoir, F. (1991) Quantitative analysis of homogeneous or stratified microvolumes applying the model “PAP”. In K.F.J. Heinrich and D.E. Newbury, Eds., *Electron Probe Quantitation*, p. 31–75. Plenum Press, New York.
- Rakovan, J.F., and Pasteris, G.D. (2015) A technological gem: Materials, medical, and environmental mineralogy of apatite. *Elements*, 11, 195–200.
- Sheldrick, G.M. (2015) Crystal structure refinement with SHELXL. *Acta Crystallographica*, C71, 3–8.
- Wang, K.L., Zhang, Y., and Naab, F.U. (2011) Calibration for IR measurements of OH in apatite. *American Mineralogist*, 96, 1392–1397.
- Wardojo, T.A., and Hwu, S.J. (1996) Chlorapatite: $\text{Ca}_5(\text{AsO}_4)_3\text{Cl}$. *Acta Crystallographica*, C52, 2959–2960.
- White, T.J., and Dong, Z. (2003) Structural derivation and crystal chemistry of apatites. *Acta Crystallographica*, B59, 1–16.
- White, T., Ferraris, C., Kim, J., and Madhavi, S. (2005) Apatite—An adaptive framework structure. In G. Ferraris and S. Merlino, Eds., *Micro- and Mesoporous Mineral Phases*, 57, p. 307–401. Reviews in Mineralogy and Geochemistry, Mineralogical Society of America, Chantilly, Virginia.
- Wilson, A.J.C. (1992) *International Tables for Crystallography Volume C*. Kluwer, Dordrecht.

MANUSCRIPT RECEIVED DECEMBER 3, 2016

MANUSCRIPT ACCEPTED JUNE 7, 2017

MANUSCRIPT HANDLED BY FABRIZIO NESTOLA